# Electrodeposition of $PbO_2$ on glassy carbon electrodes: influence of ultrasound frequency

Verónica Sáez, José González-García*, Jesús Iniesta, Angel Frías-Ferrer and Antonio Aldaz

Grupo de Electroquímica Aplicada y Electrocatálisis, Departamento de Química Física

Universidad de Alicante, Ap. Correos 99. 03080 Alicante, Spain

## ABSTRACT

The influence of the ultrasonic frequency on the electrocrystallisation of lead dioxide on glassy carbon electrodes was studied in 1 mol $dm^{-3}$ $HNO_3$ + 0.1 mol $dm^{-3}$ $Pb(NO_3)_2$ using chronoamperometry and numerical approximations of the current transients obtained. The effects of the ultrasound frequency have been compared with the effects produced by other operational variables such as electrode potential.

**Key words:** ultrasound, lead dioxide, glassy carbon electrodes, sonoelectrochemistry, electrodeposition nucleation.

## 1. Introduction

Lead dioxide electrodeposition is being an active research area [1-3], especially in the reaction mechanism analysis. Several mechanisms for lead dioxide electrodeposition involving adsorbed and/or soluble intermediates [4-15] have been proposed highlighting its complexity. This complexity is related to mass transport versus lattice incorporation kinetic control for different experimental conditions [10, 16,

* Corresponding author. Tel. +33985903855; fax +33965903537. E-mail: jose.gonzalez@ua.es

17] and to interference caused by oxygen evolution at high anodic overpotentials [18]. In this context, the use of additional techniques or approaches can be useful in order to provide more information about the process.

Sonochemistry makes use of the mechanical and chemical actions of acoustic cavitation [19] and therefore, the reactivity in sonochemistry depends on the characteristics of the bubbles. Their size and lifetime, and the content of the gaseous phase, depend on the physical properties of the medium and the parameters (amplitude and frequency) of the wave. Hence, conducting a sonochemical reaction implies that a problem with a large number of operational variables is examined and that the extreme conditions generated by cavitation can strongly modify the reaction mechanism.

A recent and useful approach has been the combination of ultrasound with electrochemistry, i. e. sonoelectrochemistry, which provides several benefits: (i) enhancement of mass transport phenomena, (ii) alteration of absorption and surface properties of the electrode, (iii) sonochemical generation of electroactive species, (iv) mechanism modifications, (v) depasivation. With this approach, it is possible to obtain mechanistic information from sonoelectroanalytical studies [20] and analyze the influence of its specific parameters such as the frequency and the ultrasonic intensity [21-23]. In this context, the use of ultrasound [24-28] and microwave [29] on the electrodeposition of lead dioxide is being currently used in order to shed light on the reaction mechanism. The influence of the ultrasonic intensity has been analysed by the authors in a previous work [30] and now in this paper we present a preliminary study of the influence of the ultrasonic frequency on the electrodeposition process of lead dioxide using the Sonoreactor® supplied by Undatim.

## 2. Experimental

The chronoamperometric curves were obtained using a Voltalab electrochemical system with a DEA 332 potentiostat and an IMT 102 electrochemical interface, connected to a PC for data acquisition and control. A glassy carbon rod CV25 (0.07 $cm^2$ electrode area) from Sofacel (Le Carbone-Lorraine) was used as a working electrode. The glassy carbon rod was sheathed by two cylinders of Teflon. The first cylinder was fitted thermally whereas the second one was fitted by pressing, providing a wide sheath. The counter electrode was a spiral wound platinum wire and the reference electrode was a saturated calomel electrode (SCE) (Radiometer, Copenhagen) connected to the electrochemical cell via a Luggin capillary.

The sonoelectrochemical reactor consisted of a jacketed Sonoreactor® (20 kHz, 100 W maximum power, diameter 68 mm, depth 84 mm) supplied by Undatim. This apparatus has the potential to operate under an "automatic mode" which allows one to search for the optimal frequency, and so ensure a maximum power transmitted to the reactor. The ultrasound power applied to the electrode was independent of the frequency.

The system was electrically isolated and was calibrated by the calorimetric method in a previous work where details about the experimental cell can be found [31]. The electrochemical system was maintained at constant temperature by introducing in the solution an additional cooling glass coil, connected in series to the jacket. In order to minimise ultrasonic field perturbations the coil was fitted to the inner wall of the sonoreactor [31]. The temperature was kept to 20ºC using a thermistor (Pt100

Thermometer 638 Pt, Crison). The ultrasound source is fitted at the bottom of the cell, so that the working electrode-ultrasound horn configuration was "face on". The separation distance, d, between the Ti stepped horn (7.07 $cm^2$ emitter area) and the surface of the glassy carbon electrode was 1 cm in all experiments.

Before each experiment, the glassy carbon electrode was polished with decreasing size alumina powder (1, 0.3 and 0.05 μm) until a mirror finish was obtained. After that, the electrode was thoroughly rinsed with ultrapure water. All solutions were prepared using ultrapure water from a Millipore Mill-Q system. Solutions 200 mL as final volume were degassed and saturated with a stream of Ar in order to keep the same amount of gas in the electrolytic cell during the experiments, and avoid possible interference caused by oxygen. A stream of Ar was also maintained on the surface of the electrolyte during the experiments. During insonation of the glassy carbon electrode, no damage was detected by visual inspection and SEM micrographs. The concentration of the solution employed for the chronoamperometry study was 0.1 mol $dm^{-3}$ lead (II) nitrate (Merck a.r.) + 1 mol $dm^{-3}$ nitric acid (Merck a.r.).

**3. Results and Discussion**

Figure 1 shows the chronoamperometric curves for $PbO_2$ deposition from Pb(II) solutions on a glassy carbon electrode recorded under ultrasonic conditions (I = 1.84 W $cm^{-2}$) and for different ultrasound frequencies at a step final potential of 1.470 V *vs* SCE. In these experimental conditions, the deposition process takes place in the nucleation control zone [16]. The kinetic parameters of electrocrystallization processes can be obtained by modelling of the experimental curves using the different models proposed in the literature. Among the different models the best agreement was obtained

for the simple progressive 3D nucleation and crystal growth model with the outward growth on a substrate base plane surface not covered by growing nuclei. The relation j vs t is [32]:

$$j = j_0 \exp\left[-\frac{\pi M^2 k N_0 A}{3\rho^2}(t-t_0)^3\right] + zFk\left[1-\exp\left[-\frac{\pi M^2 k N_0 A}{3\rho^2}(t-t_0)^3\right]\right] \quad (1)$$

This equation contains four parameters: $t_0$ (s), the induction time; $j_0$ (mA $cm^{-2}$), the current density in the induction time; k (mol $cm^{-2}$ $s^{-1}$), the growth rate constant; and $N_0A$ (nuclei $cm^{-2}$ $s^{-1}$), the three-dimensional nucleation constant. Other parameters shown in equation 1 are density, ρ (9.38 g $cm^{-3}$) and molar mass, M (239.2 g $mol^{-1}$) of lead dioxide. The optimization procedure has been carried out using 6.1 Origin program. Origin's nonlinear regression method is based on the Levenberg-Marquardt (LM) algorithm and is the most widely used algorithm in nonlinear least squares fitting. The standard way of defining the best fit is to choose the parameters so that the sum of the squares of the deviations of the theoretical curve from the experimental points for a range of independent variables is minimum. $\chi^2$ parameter gives this information, so a reduced $\chi^2$ value shows a better fit. It has been considered that the experimental data show a good fit when $\chi^2$ parameter is lower to 0.5. In our case the parameter was always lower than this limit. Figure 2 shows the relationship of these parameters with the ultrasonic frequency at several step final potentials.

As it can be seen in Figure 2, when the ultrasonic frequency increases, the kinetics parameters are weakly affected and different behaviours can be observed in this narrow region. For lower step final potential (1470 mV vs SCE), $N_0A$ and induction

time decrease and growth constant increases, becoming independent of frequency when step final potential increases (1510 mV vs SCE).

It has been stressed in literature that an enhancement of frequency should produce more hydroxyl radical (in the sonolysis of water) with lessened cavitation pressure effects (mechanical effects) [33], but its effects on the electrochemical processes are subject to discussion. The majority of studies coupling electrochemistry with ultrasound have employed low frequency high power ultrasound and have highlighted that the sole effect was the change in the apparent reversibility of the electron transfer process by promoting mass transport and when the effect of the latter is corrected for, no change in the heterogeneous rate constants for electron transfer was seen in the presence of ultrasound [34]. However, for a less reversible system, ultrasound improves the reversibility [35].

On the other hand, it has been shown that sonoelectrochemistry at higher frequency is based on distinctly different processes than those governing sonoelectrochemistry at 20-40 kHz [36]. At high frequencies, the physical nature of the phenomena occurring at the electrode-solution interface is found to be considerably different from low frequencies: the strong macroscopic acoustic streaming effect decreases and a better efficiency is obtained due to the number and timescale of cavitational events, which reaches an optimum close to 500 kHz [37]. Other works [38] stress that higher frequencies provide better yields in some electrooxidation processes although this is not straightforward to explain, since cavitation phenomena, effects of acoustic impedance, cell geometry implications, etc, all change with frequency. Cavitation is more difficult to induce at higher frequencies and, if the experiments are

performed at the same ultrasonic power, this suggests that the observed benefits are not cavitational in origin. It is associated to an effect of the shorter wavelength at the higher frequency permitting a standing wave regime to establish in the cell. In the 500-800 kHz region the distance between nodes and antinodes is only of the order of millimetres and, therefore, an increase in the number of nodes within the active region of the sonoelectrochemical reactor would produce more uniform and effective sonoelectrochemical phenomena. However, in the 20-60 kHz frequency region, the half-wavelength is the order of centimetres so that only a very limited number of nodes and antinodes span the dimensions of the cell used and the effects produced in our work can not be associated to an more uniform medium.

Keeping in mind the stage above and despite the inherent lacks of the reproducibility of the ultrasonic experiments, in our case tendencies can be observed from the results obtained. It can be seen that the ultrasonic frequency influences on the growth constant k and induction time, more notoriously at low step final potentials, where the electrodeposition process is not favoured [16, 24-27] and they become independent from the ultrasound frequency for higher step final potentials. These results are consistent with those reported early [27, 30]. This behaviour can be tentatively explained due to an increase in $OH^{\cdot}$ production with frequency [33]. A higher $OH^{\cdot}$ generation increases the OH adsorption on the electrode surface, decreasing the induction time. Once a nucleus is formed, the lead dioxide deposition is favoured onto this nucleus in front of the actives sites on carbon substrate and therefore, $N_0A$ decreases. The influence on growth constant is clear; an increase in $OH^{\cdot}$ generation favours the lead dioxide deposition for any substrate (carbon or incipient lead dioxide nuclei). In this way, at higher step final potentials or temperatures, the $OH_{ads}$

concentration is favoured by electrochemical or thermal way and the ultrasonic influence is not clearly notorious.

## 4. Conclusions

The influence of the ultrasound frequency in these experimental conditions (low frequency high power ultrasound, lead dioxide kinetics under incorporation of ions at the periphery of the expanding growth centre control) has been detected. This effect is due to the increase in $OH^{\cdot}$ generation and, therefore, OH adsorption on the surface electrode.

A larger range of frequencies is planned to be studied in order to support the tendencies presented.

## 5. Acknowledgements

The authors would like to thank Universidad de Alicante for financial support under project GR03-05.

## References

1. P. K. Shen, X. L. Wei, Electrochim. Acta 48 (2003) 1743-1747.

2. A. B. Velichenko, R. Amadelli, A. Benedetti, D. V. Girenko, S. V. Kovalyov, F. I. Danilov, J. Electrochem. Soc. 149 (2002) C445.

3. S. Abaci, K. Pekmez, T. Hökelek, A. Yildiz, J. Power Sources 534 (2002) 1.

4. M. Fleischmann, M. Liler, Trans. Faraday Soc. 54 (1958) 1370.

5. M. Fleischmann, H. R. Thirsk, Electrochim. Acta 1 (1959) 146.

6. M. Fleischmann, H. R. Thirsk, Electrochim. Acta 2 (1960) 22.

7. M. Fleischmann, J. R. Mansfield, H. R. Thirsk, H. G. E. Wilson, L. Wynne-Jones, Electrochim. Acta 12 (1967) 967.

8. H. A. Laitinen, N. H. Watkins, J. Electrochem. Soc. 123 (1976) 804.

9. S. A. Campbell, L. M. Peter, J. Electroanal. Chem. 306 (1991) 185.

10. H. Chang, D. C. Johnson, J. Electrochem. Soc. 136 (1989) 17.

11. H. Chang, D. C. Johnson, J. Electrochem. Soc. 136 (1989) 23.

12. A. B. Velichenko, D. V. Girenko, F. I. Danilov, Electrochim. Acta 40 (1995) 2803.

13. A. B. Velichenko, D. V. Girenko, F. I. Danilov, J. Electroanal. Chem. 405 (1996) 127.

14. A. C. Ramamurthy, T. Kuwana, J. Electroanal. Chem. 135 (1982) 243.

15. R. G. Barradas, A. Q. Contractor, J. Electroanal. Chem. 138 (1982) 425.

16. J. González-García, F. Gallud, J. Iniesta, M. Montiel, A. Aldaz, A. Lasia Electroanalysis 13 (2001) 1258

17. A. B. Velichenko, E. A. Baranova, D. V. Girenko, R. Amadelli, s. V. Kovalev, F. I. Danilov Russ. J. Electrochem. 39 (2003) 615.

18. J. Lee, H. Varela, S. Uhm, Y. Tak, Electrochem. Commun. 2 (2000) 646.

19. K. S. Suslick, Science 247 (1990) 1439.

20. R. G. Compton, J. L. Hardcastle, J. del Campo in Bard-Stratmann (Ed.), Encyclopedia of Electrochemistry, Volume 3, (Edited by P. Unwin) Instrumentation and Electroanalytical Chemistry, Wiley-VCH, Weinheim, 2003, Ch. 2.9.

21. D. J. Walton, S. S. Phull, A. Chyla, J. P. Lorimer, T. J. Mason, L. D. Burke, M. Murphy, R. G. Compton, J. C. Eklund, S. D. Page, J. Appl. Electrochem. 25 (1995) 1083.

22. A. Benahcene, P. Labbé, C. Pétrier, G. Reverdy, New J. Chem. 19 (1995) 989.

23. J. P. Lorimer, B. Pollet, S. S. Phull, T. J. Mason, D. J. Walton, U. Gissler Electrochim. Acta 41 (1996) 2737.

24. J. González-García, J. Iniesta, A. Aldaz, V. Montiel, New J. Chem. 22 (1998) 343.

25. J. González-García, J. Iniesta, E. Expósito, V. García-García, V. Montiel, A. Aldaz, Thin Solid Films 352 (1999) 49.

26. J. González-García, V. Montiel, G. Sánchez-Cano, A. Aldaz, Spanish Pat. 9401259.

27. J. González-García, F. Gallud, J. Iniesta, V. Montiel, A. Aldaz, A. Lasia, New J. Chem. 25 (2001) 1195.

28. A. J. Saterlay, S. J. Wilkins, K. B. Holt, J. S. Foord, R. G. Compton, F. Marken, J. Electrochem. Soc. 148 (2001) E66.

29. F. Marken, Y.-C. Tsai, A. J. Saterlay, B. A. Coles, D. Tibbetts, K. Holt, C. H. Goeting, J. S. Foord, R. G. Compton, J. Solid State Electrochem. 5 (2001) 313.

30. J. González-García, V. Sáez, J. Iniesta, V. Montiel, A. Aldaz, Electrochem. Commun. 4 (2002) 370.

31. V. Sáez, A. Frías-Ferrer, J. Iniesta, J González-García, A. Aldaz, E. Riera, Ultrason. Sonochem. submitted.

32. Y. G. Li, W. Chrzanowski, A. Lasia, J. Appl. Electrochem. 26 (1996) 843.

33. T.J. Mason, E. Cordemans in: J.-L. Luche (Ed.), Synthetic Organic Sonochemistry, Plenum, New York, 1998, Ch.8.

34. R. G. Compton, J. C. Eklund, F. Marken, T. O. Rebbitt, R. P. Akkermans, D. N. Waller, Electrochim. Acta 42(1997) 2919.

35. C. G. Jung, F. Chapelle, A. Fontana Ultrason. Sonochem. 4 (1997) 117.

36. F. J. del Campo, B. A. Coles, F. Marken, R. G. Compton, E. Cordemans, Ultrason. Sonochem. 6 (1999) 189.

37 T. J. Mason, J. P. Lorimer, D. M. Bates, Ultrasonics, 30 (1992) 1.

38. D. J. Walton, T.J. Mason in: J.-L. Luche (Ed.), Synthetic Organic Sonochemistry, Plenum, New York, 1998, pag. 285.

**Captions**

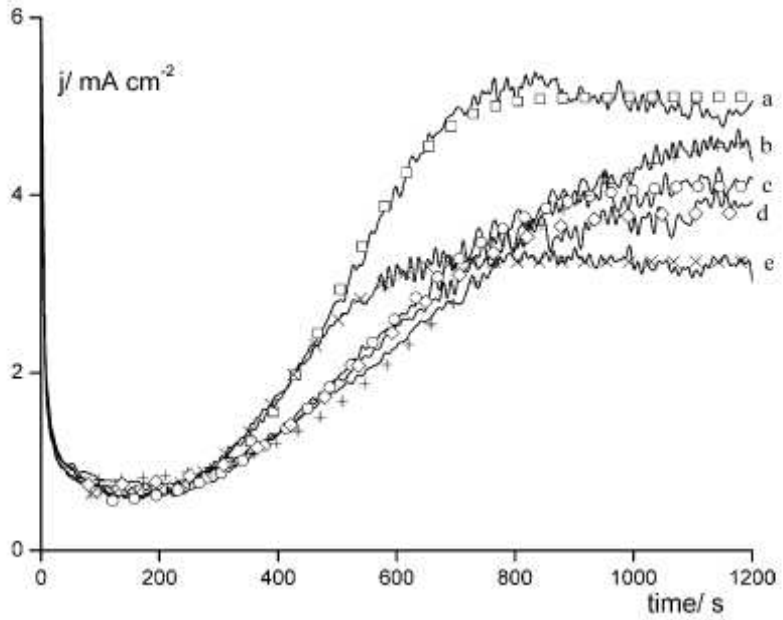


Figure 1.- Chronoamperometric curves for $PbO_2$ deposition in 0.1 mol $dm^{-3}$ $Pb(NO_3)_2$ + 1 mol $dm^{-3}$ $HNO_3$ at a glassy carbon electrode for different ultrasonic frequencies: (a) □, 20409 Hz, (b) +, 20150 Hz, (c) ○, 20169 Hz, (d) ◇, 20119 Hz, (e) ×, 20202 Hz. Electrode diammeter 3 mm. Step final potential 1450 mV vs SCE.

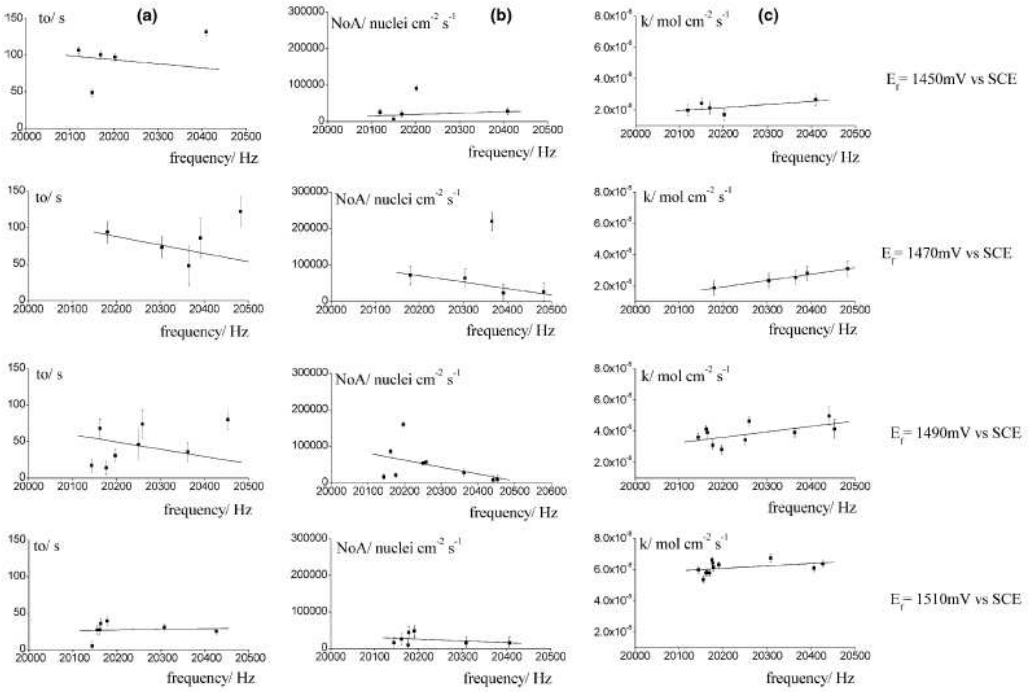

Figure 2.- Dependence of A) $t_0$, B) $N_0A$ and C) k on ultrasonic frequency for lead dioxide electrodeposition on vitreous carbon electrode.